

Relativistic Trajectories from a Configuration-Space δ -Shell Interaction*

Arthur R. Swift and Robin W. Tucker

Department of Physics and Astronomy, University of Massachusetts, Amherst, Massachusetts 01002

(Received 22 February 1971)

The Regge spectrum generated by a four-dimensional δ -shell interaction $V(r) = \lambda\delta(r-a)$, where r is the four-dimensional radius, is investigated by means of exact solutions of the Wick-rotated Bethe-Salpeter equation. In this model only the leading trajectory can generate resonances. It is infinitely rising with $\text{Im}\alpha/\text{Re}\alpha < 1$. Odd daughter trajectories either develop negative imaginary parts or do not rise. Even daughter trajectories turn over above the elastic threshold. This spectrum is contrasted with that obtained from a δ -shell interaction in potential theory. The potential-theory model is characterized by an infinite set of parallel, infinitely rising trajectories. The equivalence between the partial-wave Bethe-Salpeter equation and the continuous-dimensional formalism used here is explicitly developed. Suggestions are made for extending the method to Bethe-Salpeter equations involving spin or multichannel effects.

I. INTRODUCTION

The dynamical origin of Regge trajectories which generate infinite sequences of narrow resonances has become a subject of great interest with the mounting experimental evidence¹ that such trajectories occur in nature. Moreover, the concept of infinitely rising trajectories is central to the recent theoretical work on dual-resonance models² as well as some of the older work on bootstrap models of sequences of resonances.³ There are many approaches to this problem. Here, as in an earlier investigation of the same question,⁴ we adopt the viewpoint that Regge trajectories result from the binding of two particles by some force. We look for the forces that yield trajectories that are infinitely rising. Although this viewpoint may ultimately prove to be irrelevant for the real world, it merits investigation, since it is the most direct extrapolation of ordinary potential theory, where Regge trajectories are clearly understood. The connection between potential-theory trajectories and other approaches to defining Regge trajectories in relativistic theories is obscure, except for the fact that they both deal with singularities in the complex angular momentum plane.

Tiktopoulos⁵ and Trivedi⁶ have investigated rising trajectories in a potential-theory framework with energy-dependent potentials. They were able to obtain rising trajectories. Unfortunately, the techniques used in their investigations are not readily extended to relativistic theories. In I we investigated a variety of relativistic models. It proved difficult to generate models with rising trajectories, defined by $\text{Re}\alpha \rightarrow +\infty$, and even more difficult to generate models which lead to narrow resonances, although a suitably energy-dependent coupling constant appeared to work.

In this paper we develop another model for rising trajectories – a model based upon an energy-independent singular two-particle interaction. This work is based upon the observation that there is a class of potentials, the square well and the δ shell, which generate rising trajectories at the expense of introducing a sharp and unphysical discontinuity into the potential. Although the angular momentum barrier becomes strongly repulsive for large $\text{Re}\alpha$, the effective square-well potential

$$V_{\text{eff}}(r) = \alpha(\alpha+1)/r^2 + V(r)$$

always has a local minimum which generates resonances. The argument for the δ -shell potential is similar. Potentials which are constant in a region about the origin are known to have $|\alpha| \rightarrow \infty$ as the magnitude of the energy, $|E|$, becomes infinite.⁷ However, the behavior of $V(r)$ at the origin is not sufficient to determine the direction in which $\alpha \rightarrow \infty$. The square-well potential has been analyzed in detail,⁸ but explicit Regge trajectories for the δ -shell potential have not, to our knowledge, appeared before. In Sec. II we present a brief description of the Regge trajectories for the δ -shell potential. The pattern of trajectories that emerges constitutes the motivation for a search for the relativistic analog of the δ shell.

As before, we use the partial-wave Bethe-Salpeter equation, or an equivalent reformulation of it, to unitarize a basic interaction which we choose to be a four-dimensional δ shell upon rotation to a Euclidean four-space. At the end of the paper we discuss a possible physical interpretation of this interaction. The problem of solving the Bethe-Salpeter equation with a δ -shell interaction proves to be nontrivial and quite interesting in its own right. The three-shell is trivially soluble because the partial-wave expansion of the kernel leads to a

separable equation. An $O(4)$ expansion of the Bethe-Salpeter kernel leads to an infinite sum of separable terms. If it were not for the center-of-mass energy $2E$, which destroys the $O(4)$ invariance of the equation, the Bethe-Salpeter equation would be exactly separable. At $E=0$ it is separable and we have exact algebraic solutions with which to compare our numerical solutions. For $E \neq 0$ we must solve an infinite set of coupled algebraic equations by numerical methods. We are able to obtain the *exact* leading and secondary trajectories for energies above as well as below threshold. The method of solution along with a detailed discussion of the results is given in Sec. IV and Appendix B.

Section III of this paper deals with the extension of the continuous-dimensional approach to solving the Bethe-Salpeter equation.^{4,9} The three- and four-dimensional δ -shell interactions are used as examples of the formalism. This section may be skipped by any reader interested only in the trajectories generated by these models.

A few results of the four-shell calculations are worth mentioning here. The leading trajectory rises with a small imaginary part. However, it is not narrow-width in the sense of producing narrow-width resonances. The odd daughter trajectories are decoupled from the parent and even daughters in the equal-mass limit we consider. More interesting is the fact that rising odd daughters develop negative imaginary parts above threshold. This is the first nonperturbative dynamical calculation of these daughters above threshold and suggests that even if the odd daughters have rising real parts, they will not manifest themselves as resonances. Secondary trajectories, which in the three-shell are parallel to the leading trajectory for positive E^2 , are no longer parallel. They undergo collisions for negative E^2 and do not rise indefinitely as E^2 is increased above threshold. In fact, for the choice of parameters we investigate in detail, only the leading trajectory reaches the resonance region with a positive imaginary part. Thus, although an interpretation of the basic dynamics represented by a four-dimensional δ -shell potential is difficult, we find the results suggestive of the interesting possibility that an infinitely rising parent trajectory with resonances on it need not be accompanied by rising secondary trajectories which also generate resonances. In such a world, the secondary resonances near the ρ , f_0 , etc., resonances would not exist.

II. NONRELATIVISTIC δ -SHELL POTENTIAL

One of the simplest nonrelativistic potentials is surely the three-dimensional δ -shell potential $V(r)$

$= -g\delta(r-a)$. Indeed it appears in at least one quantum mechanics text as a pedagogical exercise in scattering theory.¹⁰ Physically it approximates a strong surface interaction between two particles. In any case, it is interesting to investigate the Regge spectrum produced by such a simple potential.

An elementary quantum-mechanics calculation shows that poles of the partial-wave scattering amplitude are given by¹⁰

$$1 = \frac{1}{2} i \pi g a J_\lambda(ka) H_\lambda^{(1)}(ka), \quad (1)$$

where $\lambda = \alpha + \frac{1}{2}$, α is the complex angular momentum, and $J_\lambda (H_\lambda^{(1)})$ is a Bessel (Hankel) function. We work in units where $k^2 = s$, the nonrelativistic center of mass-energy. To analytically continue (1) below threshold, we set k equal to $i\kappa$. In the limit $s=0$, it is possible to solve (1) exactly for the leading trajectory and obtain $\alpha(0) = -\frac{1}{2} + \frac{1}{2}ga$. If $\alpha(0) < -\frac{1}{2}$, the solutions at $s=0$ depend on the order of taking certain limits, and we find that $\alpha(0) + \frac{1}{2}$ must be a negative integer for secondary trajectories. In Fig. 1 we display $\text{Re } \alpha$ as a function of s for the leading trajectory and three secondary trajectories. Figure 2 shows the same trajectories in the complex α plane. Several properties of these trajectories are reminiscent of the properties often assumed for relativistic trajectories. All the trajectories are infinitely rising as $s \rightarrow +\infty$. In other words, $\text{Re } \alpha \rightarrow +\infty$ as $s \rightarrow +\infty$. The trajectories are nearly narrow-width in the sense that $\text{Im } \alpha / \text{Re } \alpha < 1$ (see Fig. 2). Actually, the trajectories do not generate an infinite set of narrow-width resonances due to the smallness of $d \text{Re } \alpha(s) / ds$. If a resonance of spin J has a narrow width, then

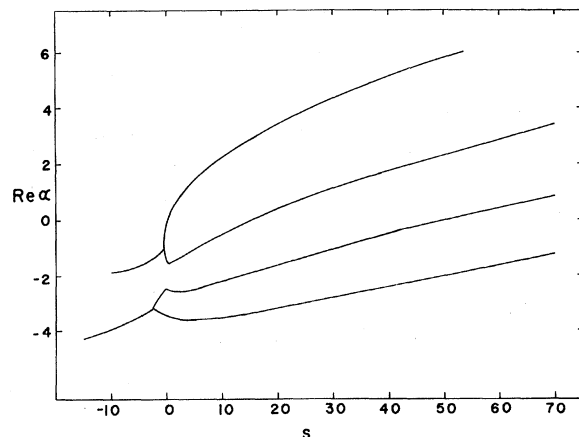


FIG. 1. $\text{Re } \alpha$ is plotted as a function of s for the leading and first three secondary trajectories generated by a three-dimensional δ -shell interaction. Both the coupling constant g and the radius of interaction a are set equal to unity. With this choice of parameters, $\alpha(0) = 0$ for the leading trajectory.

the ratio of its width to its mass, Γ/E_0 , is given in potential theory by¹¹

$$\frac{\Gamma}{E_0} = \frac{2 \operatorname{Im} \alpha(s_0) \operatorname{Re} \alpha'(s_0)}{s_0 \{ [\operatorname{Re} \alpha'(s_0)]^2 + [\operatorname{Im} \alpha'(s_0)]^2 \}}, \quad (2)$$

where $\operatorname{Re} \alpha(s_0) = J$, $\alpha' = d\alpha/ds$, and $s_0 = E_0$. For the trajectories shown in Figs. 1 and 2, this dimensionless number is typically 1.5 compared to 0.2 for the ρ resonance. For $s < 0$ the trajectories collide and recede to infinity in complex-conjugate pairs parallel to the imaginary α axis as $s \rightarrow -\infty$.

A careful consideration of the asymptotic behavior of the Bessel functions in (1) shows that the δ -shell trajectories have the asymptotic form $\alpha(s) = \pm as^{1/2}$, where a is the radius of interaction. In other words, the trajectories are independent of the coupling constant for large s . The imaginary part of α need not tend to zero or a constant, but the ratio $\operatorname{Im} \alpha / \operatorname{Re} \alpha$ vanishes for large positive s . This asymptotic form is also valid for negative s , where $\operatorname{Re} \alpha / \operatorname{Im} \alpha$ vanishes. The values of s and α in Figs. 1 and 2 are not truly asymptotic.

Not only are we able to obtain the trajectories in Figs. 1 and 2 which have nice properties, but we are also able to calculate the trajectories associated with the Gribov-Pomeranchuk condensation at threshold.¹² They are shown in Fig. 3 in the complex α plane. These trajectories approach $\operatorname{Re} \alpha = -\frac{1}{2}$ in complex-conjugate pairs as $s \rightarrow 0$ from below. Above threshold we see one manifestation of the singular nature of the δ -shell potential. Rather than moving away from $\operatorname{Re} \alpha = -\frac{1}{2}$ into the left half of the α plane, one set of the Gribov-Pomeranchuk trajectories approaches $\operatorname{Re} \alpha = +\infty$.¹¹ Inasmuch as the imaginary parts of these singular trajectories are large, they do not manifest themselves as resonances. It is worth noting that a fur-

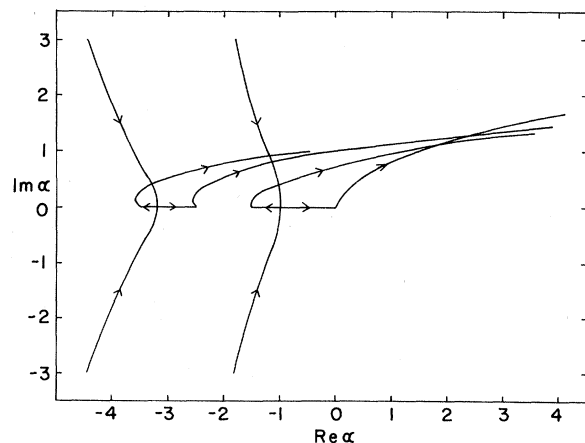


FIG. 2. The trajectories of Fig. 1 are shown in the complex α plane. The arrows indicate the direction of increasing s .

ther manifestation of the singular nature of this potential is that the asymptotic behavior of the scattering amplitude as the cosine of the scattering angle tends to infinity is not determined by the rightmost pole in the angular momentum plane.⁸

In an effort to obtain trajectories which generate narrow resonances, we have solved (1) above threshold with an energy-dependent coupling strength of the form $g = g_0(1+s)^\beta$. If $0.0 < \beta < 0.5$, both $\operatorname{Re} \alpha$ and $\operatorname{Im} \alpha$ increase indefinitely with s , but for large s the ratio $\operatorname{Im} \alpha / \operatorname{Re} \alpha$ is decreased relative to its value with $\beta = 0$. If $\beta = 0.5$, $\operatorname{Re} \alpha$ is a monotonically increasing function of s , while $\operatorname{Im} \alpha$ is asymptotically a constant. When $\beta > 0.5$, $\operatorname{Im} \alpha \rightarrow 0$ as s becomes large, and we have a truly narrow-width trajectory. This energy-dependent coupling could be viewed as a result of exchanging spin. On the other hand, if absorptive effects are included by letting g develop a positive imaginary part, $\operatorname{Im} \alpha$ is increased. These two modifications of the simple three-dimensional δ -shell interaction could be used to make a simple dynamical model of a Regge trajectory and all its secondaries. Such a model would be useful as input for calculations involving Regge cuts.

For a final amusing exercise we have calculated $\sin^2 \delta_l$, the partial-wave phase shift, as a function of energy for physical l . Asymptotically $\sin^2 \delta_l$ is an oscillating function with essentially constant amplitude. Each peak represents a secondary trajectory crossing that value of l , showing again that the trajectories occur in infinitely rising parallel families. The poles in the s plane are far

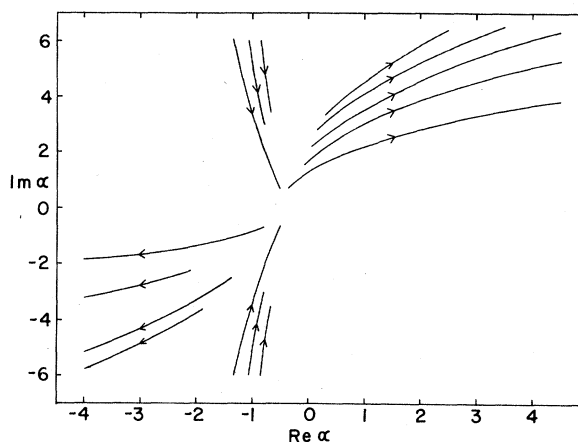


FIG. 3. The Gribov-Pomeranchuk trajectories for the nonrelativistic δ -shell interaction are shown in the complex α plane. Both g and α have the same values as in Figs. 1 and 2. For $s < 0$, these trajectories approach $\operatorname{Re} \alpha = -\frac{1}{2}$ in complex-conjugate pairs. Their imaginary parts appear not to vanish at threshold. When $s > 0$, the trajectories recede from $\operatorname{Re} \alpha = -\frac{1}{2}$ in the first and third quadrants.

from the physical region, so that the phase shift never goes through $\pi/2$, except perhaps for the very first resonance if there is a bound state with that angular momentum.

Motivated by the discovery of a potential which generates a set of infinitely rising parallel trajectories with $\text{Im}\alpha/\text{Re}\alpha$ less than unity, we seek a relativistic generalization of the three-dimensional δ -shell potential. In Sec. III we extend the formalism developed previously for the investigation of relativistic trajectories and then apply it to the four-dimensional δ -shell interaction.

III. CONTINUOUS-DIMENSIONAL TECHNIQUES AND THE FOUR-DIMENSIONAL δ SHELL

The Wick-rotated¹³ Bethe-Salpeter equation for a four-dimensional δ -shell interaction can be written down and solved without recourse to the continuous-dimensional formalism we developed in previous papers on relativistic Regge trajectories. However, the four-shell interaction offers us an opportunity to demonstrate explicitly the equivalence between working in a space of $2\alpha + 4$ dimensions,⁹ where α is to be identified with the trajectory function, and using the conventional partial-wave Bethe-Salpeter equation. One result of this digression into formalism will be an indication that our technique can be used to obtain trajectories from any system of Bethe-Salpeter equations, including those involving particles with spin.

The starting point in our development is the homogeneous Wick-rotated Bethe-Salpeter equation in momentum space. This equation describes two spinless particles with momenta p_1 and p_2 interacting to form a bound state with momentum $P = (0, iE)$. Thus we have

$$\begin{aligned} \phi(p, E) = \frac{1}{2\pi^2} \int d^4k K((p-k)^2) \\ \times G_1((k-iE)^2) G_2((k+iE)^2) \phi(k, E), \end{aligned} \quad (3)$$

where $p = \frac{1}{2}(p_1 - p_2)$. In Eq. (3) the interaction kernel $K(q^2)$ is iterated with two-particle intermediate states, and $G_i(q^2)$ is the propagator for the i th particle. The generalization of (3) to problems involving either coupled two-body channels or spinning particles is both standard and straightforward. The three-dimensional partial-wave equation corresponding to (3) is

$$\begin{aligned} f_i(p, p_0, E) = \frac{1}{\pi} \int_{-\infty}^{\infty} dk_0 \int_0^{\infty} k^2 dk K_i(p, k, (p_0 - k_0)) \\ \times G_1((k-iE)^2) G_2((k+iE)^2) f_i(k, k_0, E), \end{aligned} \quad (4)$$

where

$$\begin{aligned} f_i(p, p_0, E) \\ = \int_{-1}^1 P_l(\cos\theta) \phi(p \sin\theta, 0, p \cos\theta, p_0; E) d\cos\theta \end{aligned}$$

and

$$\begin{aligned} K_i(p, k, (p_0 - k_0)) \\ = \int_{-1}^1 dz P_l(z) K((p_0 - k_0)^2 + p^2 + k^2 - 2pkz). \end{aligned} \quad (5)$$

Rodrigues's formula for a Legendre polynomial,

$$P_l(z) = \frac{1}{2^l l!} \frac{d^l}{dz^l} (z^2 - 1)^l, \quad (6)$$

can be used to obtain the continuation of (5) into the complex l plane. Using (6) in (5) and integrating by parts l times, we obtain

$$K_l = \frac{1}{2^l l!} \int_{-1}^1 dz (1-z^2)^l \frac{d^l}{dz^l} K((p-k)^2). \quad (7)$$

In terms of an element of surface on a $(2l+3)$ -dimensional sphere, Eq. (7) can be written in the form

$$K_l = \frac{p^l k^l}{2\pi^{2l+3}} \int_{\Omega} \bar{K}_l((p-k)^2) d\Omega_{2l+3}, \quad (8)$$

where

$$\bar{K}_l(\tau) = (-1)^l \frac{d^l}{d\tau^l} K(\tau). \quad (9)$$

$\bar{K}_l(\tau)$ is a function of the invariant $\tau = (p-k)^2$ and is to be identified with the l -dependent kernel in I which was defined by

$$\bar{K}_l(\tau) = \frac{1}{\Gamma(-l)} \int_0^{\infty} y^{-l-1} K(y+\tau) dy. \quad (10)$$

From (10) we have $\bar{K}_0(\tau) = K(\tau)$ and

$$(-1)^l \frac{d^l}{d\tau^l} \bar{K}_\alpha(\tau) = \bar{K}_{\alpha+l}(\tau). \quad (11)$$

Setting $\alpha = 0$ in (11) completes the identification of (10) and (9). Returning to the partial-wave Bethe-Salpeter equation, we substitute (8) into (4) to obtain

$$\begin{aligned} F_i(p, p_0, E) = \frac{1}{2\pi^{2l+3}} \int_0^{\infty} k^{2l+3} dk \int_{\Omega} d\Omega_{2l+3} \bar{K}_l((p-k)^2) \\ \times G_1((k-iE)^2) G_2((k+iE)^2) F_i(k, k_0, E), \end{aligned} \quad (12)$$

where

$$p^l F_i(p, p_0, E) = f_i(p, p_0, E).$$

Now, by regarding the physical four-space of vec-

tors (p, p_0) as a subspace of an r -dimensional auxiliary space into which the physical vectors can rotate, we obtain the continuous-dimensional equation previously derived by more devious means⁹:

$$F_l(p, E) = \frac{1}{2\pi^{l+2}} \int d^{2l+4} k \tilde{K}_l((p-k)^2) \times G_1((k-iE)^2) G_2((k+iE)^2) F_l(k, E). \quad (13)$$

If we perform a partial-wave expansion in $2l+3$ dimensions, the generalized S-wave equation is just the partial-wave Bethe-Salpeter equation. Once again we emphasize that the advantage of using (13) over (4) is that the kernel of the integral equation is a function of invariants. The invariant kernel can be accurately approximated by a set of finite-rank kernels in a way that leads to a straightforward calculation of Regge trajectories above as well as below the elastic threshold.

To extend the formalism to problems involving spinning particles, it is only necessary to note that the partial-wave decomposition of any Bethe-Salpeter equation leads to a set of coupled equations. The kernels in such a set of equations can always be written in a form analogous to (5). Then the appropriate separable approximation to $\tilde{K}_l((p-k)^2)$ under the integral in (8) should generate a good separable approximation to the partial-wave kernels. All that is necessary is to carry out the trivial angular integration in (8).

We show in Appendix A that $\tilde{K}_l(\tau)$, defined either by (9) or by (10), is also proportional to the $(2l+4)$ -dimensional Fourier transform of the configuration-space potential corresponding to $K(q^2)$.

As an example of this alternate approach to the partial-wave analysis of the Bethe-Salpeter equation we consider the simplest possible problem - the three-dimensional δ -shell potential in the Lippmann-Schwinger integral equation. The interaction kernel is given by the Fourier transform of the potential

$$K(q^2) = \frac{g}{4\pi} \int e^{i\vec{q}\cdot\vec{x}} \delta(r-a) d^3x = g a^2 (\frac{1}{2}\pi)^{1/2} \frac{J_{1/2}(aq)}{(aq)^{1/2}}, \quad (14)$$

where $J_\nu(z)$ is a Bessel function. The transformed kernel $\tilde{K}_l(q^2)$ obtained by means of (9) is

$$\begin{aligned} \tilde{K}_l(q^2) &= (-1)^l (\frac{1}{2}a^2)^l g a^2 (\frac{1}{2}\pi)^{1/2} \left(\frac{1}{x} \frac{d}{dx} \right) \left(\frac{J_{l+1/2}(x)}{x^{l+1/2}} \right) \Big|_{x=aq} \\ &= g a^2 (\frac{1}{2}\pi)^{1/2} (\frac{1}{2}a^2)^l \frac{J_{l+1/2}(aq)}{(aq)^{l+1/2}}. \end{aligned} \quad (15)$$

The corresponding integral equation is

$$F_l(p, x) = \frac{1}{2\pi^{l+2}} \int \frac{d^{2l+3} k \tilde{K}_l((p-k)^2)}{k^2 - s} F_l(k, s). \quad (16)$$

If we make the separable approximation

$$\tilde{K}_l((p-k)^2) \approx \frac{\tilde{K}_l(p^2) \tilde{K}_l(k^2)}{\tilde{K}_l(0)}, \quad (17)$$

Eq. (16) becomes

$$F_l(p, s) = g a^2 \sqrt{\pi} (a^2)^l \Gamma(l + \frac{3}{2}) \frac{J_{l+1/2}(ap)}{(ap)^{l+1/2}} \times \frac{1}{2\pi^{l+2}} \int d^{2l+3} k \frac{J_{l+1/2}(ak)}{(ak)^{l+1/2}} \frac{F_l(k, s)}{k^2 - s}. \quad (18)$$

The eigenvalues of (18), or the Regge trajectories, are determined by

$$1 = \frac{g a \sqrt{\pi} \Gamma(l + \frac{3}{2})}{\pi^l} \frac{2\pi^{l+3/2}}{\Gamma(l + \frac{3}{2})} \int_0^\infty \frac{k dk [J_{l+1/2}(ka)]^2}{k^2 - s} = g a I_{l+1/2}(a\sqrt{-s}) K_{l+1/2}(a\sqrt{-s}), \quad (19)$$

where $K_\nu(z)$ and $I_\nu(z)$ are modified Bessel functions. Equation (19) is the continuation of (1) to negative energies. Indeed, in this case, the separable approximation works well. The reason, of course, is that the partial-wave equation for the scattering amplitude is exactly separable when solved by conventional means. In other words, the corrections to the approximation in (17) do not contribute to (16) in the generalized S wave.

Encouraged by the three-shell potential, we turn to the four-dimensional δ shell, $V(r) = g^2 \delta(r-a)$, where r is the four-dimensional radius. Taking the four-dimensional Fourier transform of this potential, we find

$$K(q^2) = 4\pi^2 a^3 g^2 \frac{J_1(aq)}{aq}. \quad (20)$$

We are working with the Wick-rotated Bethe-Salpeter equation so that the potential $V(r)$ and the kernel $K(q^2)$ are defined in an Euclidean space. Since $K(q^2)$ is needed only for spacelike values of q^2 , we do not make any statement about its behavior for timelike q^2 in a Lorentz metric. The simplest, but by no means unique or analytic, choice would be to define $K(q^2) = 0$ for $q^2 < 0$. Since we solve the integral equation in a region free from singularities and then analytically continue the solutions, we are confident that the Wick rotation of contour is legitimate.¹⁴

The transformed kernel corresponding to (20) is

$$\tilde{K}_l(q^2) = 4\pi^2 a^3 g^2 (\frac{1}{2}a^2)^l \frac{J_{l+1}(aq)}{(aq)^{l+1}}. \quad (21)$$

Inasmuch as we are interested in exact solutions for the trajectory functions, and the Bethe-Salpeter equation is not exactly separable except at $E=0$, we expand $\tilde{K}_l(q^2)$ in partial waves in a $(2l+4)$ -dimensional space, not a $(2l+3)$ -dimensional one.

This expansion is useful for this particular kernel since it leads to an infinite sum of separable terms,¹⁵

$$\begin{aligned} \tilde{K}_l((p-k)^2) &= 4\pi\alpha^3 g^2 (\frac{1}{2}\alpha^2)^{l+1} 2^{l+1} \Gamma(1+l) \\ &\times \sum_{n=0}^{\infty} (n+l+1) \frac{J_{n+l+1}(ak)}{(ak)^{l+1}} \frac{J_{n+l+1}(ap)}{(ap)^{l+1}} \\ &\times C_n^{l+1}(\cos\theta_{pk}), \end{aligned} \quad (22)$$

where $p \cdot k = pk \cos\theta_{pk}$, and p and k are $(2l+4)$ -dimensional vectors. Equation (22) is to be used in (13). The Gegenbauer function satisfies an addition theorem of the form¹⁶

$$\begin{aligned} C_n^{l+1}(\cos\theta_{pk}) &= N_n \sum_{m_i} Y_{nm_1} \dots (\Omega_p) Y_{nm_1}^* \dots (\Omega_k) \\ &= \frac{n! \Gamma(2l+2)}{\Gamma(2l+2+n)} C_n^{l+1}(\cos\theta_p) C_n^{l+1}(\cos\theta_k) + \dots \end{aligned} \quad (23)$$

$Y_{nm_1 m_2 \dots m_r}$ is a generalized spherical harmonic in $r+2=2l+4$ dimensions. In the second line of (23) the terms represented by the dots vanish in the generalized S -wave limit. Using (22) and (23) in (13) and keeping just the S -wave term, we obtain the following form of the Bethe-Salpeter equation for the four-dimensional δ -shell potential:

$$\begin{aligned} F_l(p, \cos\alpha) &= 8\pi^{3/2} \alpha g^2 \frac{\Gamma(l+1)}{\Gamma(l+\frac{3}{2})} \sum_{n=0}^{\infty} \frac{(l+1+n)n! \Gamma(2l+2)}{\Gamma(2l+2+n)} \frac{J_{l+1+n}(ap)}{p^{l+1}} C_n^{l+1}(\cos\alpha) \\ &\times \left\{ \int_0^{\infty} k^{2l+3} dk \int_0^{\pi} \frac{d\beta (\sin\beta)^{2l+2} C_n^{l+1}(\cos\beta)}{(k^2 + \mu^2 - E^2)^2 + 4E^2 k^2 \cos^2\beta} \frac{J_{l+1+n}(ak)}{k^{l+1}} F_l(k, \cos\beta) \right\}. \end{aligned} \quad (24)$$

The denominator factor in the integral comes from the product of the propagators for two equal-mass particles. Since the term in curly brackets is a constant independent of p and $\cos\alpha$, the eigenvalue condition is reduced to the problem of finding the zeros of the infinite determinant

$$\det[1 - \Omega(l)S(l, E)] = 0, \quad (25)$$

where $S(l, E)$ is an infinite symmetric matrix whose elements are given by

$$\begin{aligned} S_{mn} &= \int_0^{\infty} k dk \int_{-1}^1 dz (1-z^2)^{l+1/2} \\ &\times \frac{J_{l+1+m}(ak) J_{l+1+n}(ak)}{(k^2 + \mu^2 - E^2)^2 + 4E^2 k^2 z^2} C_m^{l+1}(z) C_n^{l+1}(z). \end{aligned} \quad (26)$$

Moreover,

$$\Omega_{mn} = \frac{4G^2 m!}{\sqrt{\pi} \alpha^2} (l+1+m) \frac{\Gamma(l+1)}{\Gamma(l+\frac{3}{2})} \frac{\Gamma(2l+2)}{\Gamma(2l+2+m)}. \quad (27)$$

We have introduced a dimensionless coupling constant $G^2 = 2\pi^2 \alpha^3 g^2$.

In Sec. IV we solve (25) by approximating $S(l, E)$ by a finite matrix and then expanding the order of the matrix until the solutions are stationary. Here we make several general comments about the infinite system of coupled algebraic equations. As a consequence of using equal masses in the problem, the integrand in (26) has a definite parity under $z \rightarrow -z$. This means that S_{mn} is zero unless $m+n$ is even. Hence, we have two uncoupled infinite determinants to solve. One determinant contains the leading trajectory and all even daughters, while the other contains the odd daughter trajectories

which are decoupled from the even trajectories and the mass-shell elastic scattering amplitude in the equal-mass limit. Next, we note that when $E=0$, S_{mn} vanishes (unless $m=n$) due to the orthogonality of the Gegenbauer functions. At $E=0$, we find that $\Omega_{nn} S_{nn}(l, 0) = \Omega_{00} S_{00}(l+n, 0)$, indicating that the trajectories occur in Toller families¹⁷ as is to be expected. Moreover, at $E=0$, and presumably near $E=0$, the leading trajectory is given by S_{00} ; the leading trajectory and first even daughter are contained in the 2×2 approximation to the full matrix, and so forth. This progression forms the basis for our approach to solving (25) for all energies. In Sec. IV we use the $E=0$ equation as a check on our results for $E \neq 0$.

Finally, we note that the approximation used in solving (25) appears to be very similar to the finite-rank method recently developed by Kershaw, Snodgrass, and Zemach¹⁸ for solving the Bethe-Salpeter equation. There is a very important difference, however. They work with the configuration-space Bethe-Salpeter equation. Their amplitude has the direct particle propagators removed from it, so that its $O(4)$ expansion is different from that for our amplitude. Their approach fails at the elastic threshold, while ours converges extremely rapidly above threshold. In fact, we initially attempted to apply their formalism to this problem and found numerical results for the Regge trajectories which were unsatisfactory even near $E=0$.

IV. RESULTS AND CONCLUSIONS

As mentioned in Sec. III, the eigenvalue condition (25) simplifies considerably at $E=0$. Not only

does $S(l, E)$ become a diagonal matrix, but also the double integral in (26) can be carried out analytically to give¹⁹

$$S_{mn} = \frac{\pi \Gamma(2l+2+n)}{n!(n+l+1)[\Gamma(1+l)]^2} \frac{a^2}{2^{2l+3}(l+1+n)} \times [I_{l+n}(a\mu)K_{l+n}(a\mu) - I_{l+n+2}(a\mu)K_{l+n+2}(a\mu)]. \quad (28)$$

Upon multiplication by Ω_{mn} , (28) leads to the following expression for the $E=0$ intercepts of the trajectories:

$$1 = \frac{G^2}{l+n+1} [I_{l+n}(a\mu)K_{l+n}(a\mu) - I_{l+n+2}(a\mu)K_{l+n+2}(a\mu)]. \quad (29)$$

Each trajectory determined by (29) with $n=0$ is accompanied by an infinite set of integrally space secondary trajectories. There may exist additional trajectories at the negative integers whose $E=0$ intercepts are not given by (29) just as there are such trajectories for the three-dimensional δ shell.

In Appendix B we show that the k integral in (26) can be performed for $E \neq 0$ and the z integral folded onto the interval 0 to 1. Hence, for $E \neq 0$ we need to calculate a one-dimensional integral over a finite range and we do not have to resort to the Blankenbecler-Sugar²⁰ approximation. In Appendix B we also discuss the analytic continuation of the integral representation of S_{mn} above the elastic threshold at $E = \mu$ and below $\text{Re}l = -\frac{3}{2}$, where the

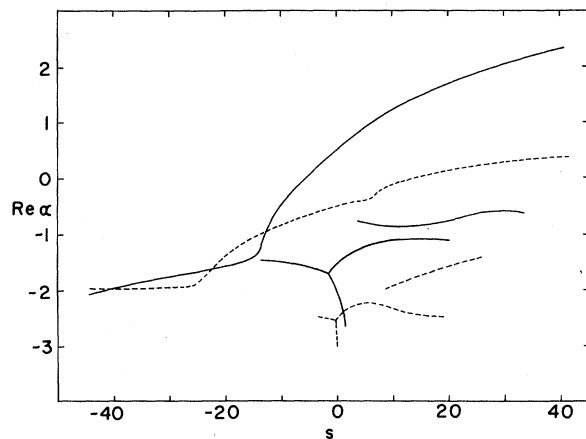


FIG. 4. $\text{Re} \alpha$ is plotted as a function of s for the leading and seven secondary trajectories generated by the relativistic δ -shell interaction with $G^2 = 6.0$, $a = 1.0$, and $\mu = 1.0$, where μ is the direct mass. The coupling constant is fixed by the requirement that $\alpha(0) = 0.5$ for the leading trajectory. In these units threshold occurs at $s = 4.0$. The solid trajectories are those coupled to the leading trajectory in the equal-mass limit; the dashed trajectories are decoupled and include the odd daughters. At $s = 0$, the leading trajectory and the kinematically constrained daughters are integer-spaced.

integral diverges because of the factor $(1-z^2)^{l+1/2}$. In both cases the continuations are straightforward though in practice the algebra becomes complicated.

In Figs. 4 and 5 we display the Regge trajectories calculated with this four-dimensional δ -shell interaction. In Fig. 4 we plot $\text{Re} \alpha$ as a function of $s = 4E^2$ while in Fig. 5 the trajectories are drawn in the complex l plane. We have calculated those trajectories which have $\text{Re} \alpha > -3$ in the region $-40 < s < +40$ in units where the direct particle has mass $\mu = 1.0$ and threshold is at $s = 4.0$. We normalize the leading trajectory to $\alpha(0) = 0.5$. The leading trajectory calculated from S_{00} alone is indistinguishable from the leading trajectory calculated either from the 2×2 or the 3×3 approximations to $S(l, E)$ over the range $-20 < s < +40$. In the range $-40 < s < -20$, the 2×2 and 3×3 approximations are indistinguishable. This rapid convergence carries over to the secondary trajectories and suggests that all trajectories could be calculated with reasonable accuracy from the diagonal elements of $S(l, E)$ alone.

One of the most striking features of the trajectories in this model is that the leading trajectory appears to be infinitely rising. Just as in the three-shell, this trajectory has $\text{Im} \alpha / \text{Re} \alpha < 1$ so that it is narrow compared to the relativistic trajectories investigated in detail in I. For relativistic trajectories the ratio of width to energy is given by (2) divided by 2 with s the square of the center-of-mass energy. This ratio varies from 0.54 at $s = 21$ to 0.63 at $s = 37$ compared to 0.2 for the ρ resonance. The second important fact about these trajectories

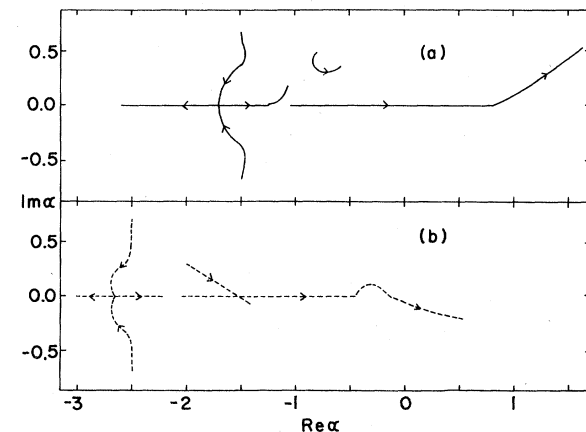


FIG. 5. The trajectories of Fig. 4 are shown in the complex l plane. The even trajectories are in (a) while the odd ones are in (b). Again the arrows indicate the direction of increasing s . The imaginary part of the third daughter [identified by $\alpha(0) = -2.5$] above threshold is too small to be shown. For clarity the leading trajectory is not shown for $s < -13$; it is real in this region.

is that the odd rising daughters develop negative imaginary parts above threshold. This is the first dynamical calculation of daughter trajectories above threshold, and it suggests that the odd daughter trajectories do not manifest themselves as resonances even if their real parts reach the physical region of $\text{Re}l \geq 0$. The third interesting feature of these solutions is that all trajectories, except the leading one and the first daughter, undergo collisions and move off into the complex l plane as s is decreased from $s=0$. The trajectories which collide with the kinematically constrained daughters pass through negative integers at $s=0$ and drop very rapidly as s increases above $s=0$. The leading trajectory, which appears to fall indefinitely, and the first daughter cross for negative s . In an unequal-mass calculation, where the even and odd trajectories are coupled, the crossing point becomes a collision, and the trajectories will make an excursion into the complex l plane.

The even daughter pole which has $\alpha(0) = -1.5$ does not rise above $\text{Re}l = -1.0$. This behavior puzzles us. The trajectory starting at $\alpha(0) = -2.5$ does not cross $\text{Re}\alpha = -2.0$. In both cases there are trajectories lying above these daughter trajectories which are not kinematically constrained at $s=0$. Apparently, either negative integer values of $\text{Re}l$ or these extra secondary trajectories act as barriers in the l plane. This effect is stable under increasing the dimensionality of $S(l, E)$. We are unable to track these extra trajectories below the elastic threshold. The fact that their imaginary parts do not vanish at threshold suggests that these trajectories may be associated with a relativistic version of the Gribov-Pomeranchuk threshold condensation.¹¹ There probably exist numerous other trajectories of this type, but we have not made an exhaustive search for them. One complication in understanding this barrier phenomenon and the associated trajectories is the exceeding sensitivity of the eigenvalue equation (25) to small changes in either $\text{Re}l$ or $\text{Im}l$ when s is large.

In summary, the important feature of this simple dynamical model is that it generates an infinitely rising leading trajectory. With the possible exception of the first daughter trajectory, none of the secondary trajectories approach the region $\text{Re}l > 0$. The odd rising daughter trajectories develop negative imaginary parts above threshold. A complicated pattern of colliding trajectories exists for $s < 0$. These results suggest the possibility that even if there exist infinitely rising trajectories in nature, the existence of daughter poles near $s=0$ does not imply that there should exist a set of parallel secondary trajectories also generating resonances. Such a possibility would contradict the world picture emerg-

ing from dual-resonance models.²

We end this paper by briefly discussing the question of just what sort of an interaction is represented by a four-dimensional δ shell in the Euclidean continuation of the Bethe-Salpeter equation. The straightforward analytic continuation of the Bessel function in (20) to timelike values of q^2 leads to serious divergence difficulties in the generalized ladder-diagram series represented by the Bethe-Salpeter equation in the Lorentz metric. One possible answer to this question is given by asking for the nonrelativistic potential which yields the Born approximation (20). Such an approach is one way of relating the Yukawa potential to single-particle exchange. We do this and find the nonrelativistic potential corresponding to (20) is

$$V(r) = -\frac{8\pi ag^2}{(a^2 - r^2)^{1/2}}, \quad r < a \quad (30)$$

$$V(r) = 0, \quad r > a.$$

This attractive potential is finite at the origin, infinite at $r=a$, and zero for $r>a$ —not an unreasonable potential to describe a strong surface interaction between two particles. It is certainly less singular than the three-dimensional δ -shell potential.

ACKNOWLEDGMENTS

We gratefully acknowledge the generous support of a University of Massachusetts Research Computing Grant which made our numerical analysis possible. One of us (A. R. S.) would like to thank the Aspen Center for Physics for its hospitality during the initial investigation into the three-dimensional δ shell.

APPENDIX A

We show that the Euclidean Fourier transform in $2\alpha + 4$ dimensions of an invariant (α -independent) configuration-space potential $V(r)$ is proportional to the transformed kernel $\bar{K}_\alpha(q^2)$ defined by Eq. (10). The four-dimensional kernel $K(q^2)$ can be used to define a configuration space potential $V(r)$ by the relation

$$\begin{aligned} K(q^2) &= \frac{1}{(2\pi)^2} \int_{-\infty}^{\infty} V(r) e^{-i q \cdot x} d^4x \\ &= \int_0^{\infty} V(r) \frac{J_{\alpha+1}(qr)}{q} r^2 dr. \end{aligned} \quad (A1)$$

If (A1) is inserted into (10), we obtain another representation for $\bar{K}_\alpha(q^2)$:

$$\bar{K}_\alpha(q^2) = \frac{1}{2^\alpha} \int_0^{\infty} \frac{J_{\alpha+1}(rq)}{(rq)^{\alpha+1}} V(r) r^{2\alpha+3} dr. \quad (A2)$$

On the other hand, if we regard r as the $(2\alpha+4)$ -dimensional invariant length in that space, we can calculate the Fourier transform

$$\begin{aligned}\tilde{K}_\alpha(q^2) &= \frac{1}{(2\pi)^\alpha} \int_{-\infty}^{\infty} V(r) e^{-iq \cdot x} d^{2\alpha+4}x \\ &= \int_0^\infty r^{2\alpha+3} \frac{J_{\alpha+1}(qr)}{(qr)^{\alpha+1}} V(r) dr.\end{aligned}\quad (\text{A3})$$

Hence, we have the result

$$\bar{K}_\alpha(q^2) = \frac{1}{(4\pi)^\alpha} \int_{-\infty}^{\infty} V(r) e^{-iq \cdot x} d^{2\alpha+4}x.$$

APPENDIX B

In this appendix we perform the k integration involved in the definition of S_{mn} , Eq. (26), and then analytically continue the result above the elastic threshold at $E = \mu$. We define

$$I_{mn} = \int_0^\infty k dk \frac{J_{\mu+n}(ak) J_{\mu+m}(ak)}{(k^2 + \mu^2 - E^2)^2 + 4E^2 k^2 \cos^2 \beta}.\quad (\text{B1})$$

Since I_{mn} is symmetric, we choose $m \leq n$ and utilize the relation²¹

$$I_{\mu+m}(z) = (1/i\pi) [e^{-i\pi(\mu+m)} K_{\mu+m}(z) - K_{\mu+m}(-z)],\quad (\text{B2})$$

so that with the change of variable $k = iz$, we obtain for $n - m$ even

$$I_{mn} = \frac{(-1)^{(n-m)/2}}{i\pi} \int_{-i\infty}^{i\infty} z dz \frac{I_{\mu+n}(az) K_{\mu+m}(az)}{(\mu^2 - E^2 - z^2)^2 - E^2 z^2 \cos^2 \beta}.\quad (\text{B3})$$

The integrand has poles at

$$\begin{aligned}z_{1,2} &= \pm E \cos \beta + (\mu^2 - E^2 \sin^2 \beta)^{1/2} - i\epsilon, \\ z_{3,4} &= \pm E \cos \beta - (\mu^2 - E^2 \sin^2 \beta)^{1/2} + i\epsilon,\end{aligned}\quad (\text{B4})$$

and a cut along the negative z axis. With $n \geq m$ there is no singularity at $z = 0$. Closing the contour on the right we obtain the result

$$\begin{aligned}I_{mn} &= \frac{(-1)^{(n-m)/2}}{4E \cos \beta} \frac{1}{(\mu^2 - E^2 \sin^2 \beta)^{1/2}} \\ &\quad \times [I_{\mu+n}(az_1) K_{\mu+m}(az_1) - I_{\mu+n}(az_2) K_{\mu+m}(az_2)].\end{aligned}\quad (\text{B5})$$

In order to analytically continue this expression above threshold, we rotate the roots z_1 and z_2

away from the cuts of the Bessel functions by means of the relations

$$\begin{aligned}I_\mu(az_2) &= e^{-i\pi\mu} I_\mu(-az_2), \\ K_\mu(az_2) &= i\pi I_\mu(-az_2) + e^{i\pi\mu} K_\mu(-az_2).\end{aligned}\quad (\text{B6})$$

This ensures that as β varies from 0 to π the roots z_1 and z_2 are positive and, therefore, in a singularity-free domain.

The final result for the matrix element in terms of $z = \cos \beta$ is

$$\begin{aligned}S_{mn} &= (-1)^{(n-m)/2+1} \int_0^1 \frac{(1-z^2)^{\alpha+1/2} dz}{2Ez(E^2 z^2 - q^2)^{1/2}} \\ &\quad \times C_m^{1+\alpha}(z) C_n^{1+\alpha}(z) L_{mn}(z, \alpha),\end{aligned}\quad (\text{B7})$$

where $q^2 = E^2 - \mu^2$ and, for $E < \mu$,

$$\begin{aligned}L_{mn}(z, \alpha) &= I_{1+\alpha+n}(az_1) K_{1+\alpha+m}(az_1) \\ &\quad - I_{1+\alpha+n}(az_2) K_{1+\alpha+m}(az_2),\end{aligned}\quad (\text{B8})$$

while for $E > \mu$,

$$\begin{aligned}L_{mn}(z, \alpha) &= I_{1+\alpha+n}(az_1) K_{1+\alpha+m}(az_1) \\ &\quad - I_{1+\alpha+n}(-az_2) K_{1+\alpha+m}(-az_2) \\ &\quad - i\pi e^{-i\pi(1+\alpha+n)} K_{1+\alpha+n}(-az_2) I_{1+\alpha+m}(-az_2).\end{aligned}\quad (\text{B9})$$

When $E^2 z^2 < q^2$, $(E^2 z^2 - q^2)^{1/2}$ is to be replaced by $-i(q^2 - E^2 z^2)^{1/2}$.

The z integral in (B7) diverges for $\text{Re } \alpha \leq -\frac{3}{2}$. The integral is analytically continued by writing

$$S_{mn} = \int_0^1 (1-z^2)^{\alpha+1/2} C_m^{1+\alpha}(z) C_n^{1+\alpha}(z) G(z, \alpha) dz,\quad (\text{B10})$$

and expanding $G(z, \alpha)$ about $z = 1$. If we define

$$G_R(z, \alpha) = \sum_{r=0}^R \frac{(z-1)^r}{r!} \frac{d^r}{dz^r} G(z, \alpha) \Big|_{z=1},\quad (\text{B11})$$

Then (B10) becomes

$$\begin{aligned}S_{mn} &= \int_0^1 (1-z^2)^{\alpha+1/2} C_m^{1+\alpha}(z) C_n^{1+\alpha}(z) [G(z, \alpha) - G_R(z, \alpha)] dz \\ &\quad + \sum_{r=0}^R \frac{1}{r!} \frac{d^r}{dz^r} G(z, \alpha) \Big|_{z=1} \int_0^1 (1-z^2)^{\alpha+1/2} C_m^{1+\alpha}(z) C_n^{1+\alpha}(z) (z-1)^r dz.\end{aligned}\quad (\text{B12})$$

The first integral now converges if $\text{Re } \alpha \leq -\frac{3}{2} - R - 1$, and the counter terms can be explicitly evaluated and then analytically continued to all values of α .

*Supported in part by the National Science Foundation.

¹V. Barger, M. Olsson, and D. D. Reeder, Nucl. Phys. B5, 411 (1968); C. B. Chiu, S. Y. Chu, and L. L. Wang, Phys. Rev. 161, 1563 (1967); V. Barger and D. Cline, Phys. Letters 27B, 321 (1968); Phys. Rev. 155, 1792 (1967).

²D. Sivers and J. Yellin, Rev. Mod. Phys. 43, 125 (1971).

³P. Carruthers and M. M. Nieto, Phys. Rev. 163, 1646 (1967); E. Golowich, *ibid.* 168, 1745 (1968).

⁴A. R. Swift and R. W. Tucker, Phys. Rev. D 2, 2486 (1970). Hereafter referred to as I.

⁵G. Tiktopoulos, Phys. Letters 28B, 185 (1969).

⁶U. Trivedi, Phys. Rev. 188, 2241 (1969).

⁷R. G. Newton, in *Proceedings of the International School of Physics "Enrico Fermi"* (Academic, New York, 1964), p. 106.

⁸A. O. Barut and F. Calogero, Phys. Rev. 128, 1383 (1962); C. G. Bollini and J. J. Giambiagi, Nuovo Cimento 28, 341 (1963).

⁹A. R. Swift and R. W. Tucker, Phys. Rev. D 1, 2894 (1970); 2, 397 (1970).

¹⁰K. Gottfried, *Quantum Mechanics* (Benjamin, New York, 1966), p. 131.

¹¹R. G. Newton, *The Complex j Plane* (Benjamin, New

York, 1964), Chap. 9.

¹²R. J. Eden, P. V. Landshoff, D. I. Olive, and J. C. Polkinghorne, *The Analytic S Matrix* (Cambridge Univ. Press, Cambridge, England, 1966), p. 158.

¹³G. C. Wick, Phys. Rev. 96, 1124 (1954).

¹⁴G. Domokos, P. Suranyi, and A. Vancure, Nucl. Phys. 60, 1 (1964).

¹⁵*Handbook of Mathematical Functions*, edited by M. Abramowitz and I. A. Stegun (U.S. G.P.O., Washington, D.C., 1964), p. 363.

¹⁶Bateman Manuscript Project, *Higher Transcendental Functions*, edited by A. Erdélyi (McGraw-Hill, New York, 1953), Vol. II, Chap. 11.

¹⁷M. Toller, CERN Reports Nos. CERN-TH-770 and 780, 1967 (unpublished); G. Domokos, Phys. Rev. 159, 1387 (1967).

¹⁸D. Kershaw, H. Snodgrass, and C. Zemach, Phys. Rev. D 2, 2806 (1970).

¹⁹I. S. Gradshteyn and I. M. Ryzhik, *Tables of Integrals, Series, and Products* (Academic, New York, 1965), pp. 679 and 694.

²⁰R. Blankenbecler and R. Sugar, Phys. Rev. 142, 1051 (1966).

²¹Reference 15, p. 376.